Indian J. Met. Geophys. (1972), 23, 1, 83-90

551. 521. 3 : 551. 508. 2 : 551. 509. 313 (547. 1)

A comparative study of radiometrically observed and numerically computed infra-red fluxes

R. R. KELKAR and R. V. GODBOLE

Indian Institute of Tropical Meteorology, Poona

(*Received 4 June 1971*)

ABSTRACT. Infra-red radiative fluxes and cooling rates obtained from radiometer soundings made over Poona during 1963-66 have been compared with the results of computations using numerical methods.

Good agreement has been noticed between the observed and computed values of the upward flux. The nature of variation with height and season of the observed and computed downward flux is found to be similar. However, at any level, the absolute value of the observed downward flux is higher than the computed one by 75 to 150 ly/day. The differences between the observed and computed values of the cooling rate are small in the troposphere.

1. Introduction

During the last decade, efforts towards the development of sophisticated numerical schemes for computing infra-red radiative fluxes in the atmosphere have moved almost in parallel with attempts to improve upon the efficiency of direct radiometer sounding techniques. In the computational methods, the major difficulties yet to be overcome are the numerical modelling of the aerosol structure of the atmosphere and the presence of clouds. Besides, numerical evaluation of infra-red flux at any level requires the knowledge of absorber concentration both above and below the level, and is therefore influenced by uncertainties of data at higher levels. On the other hand, the radiometersondes, which are useful for nocturnal measurements of infra-red flux, present difficulties during daytime because of the presence of solar radiation. However, until the radiometersonde network becomes sufficiently well-knit, numerical methods will have to be relied upon for most purposes. It is therefore desirable to make a comparative study of infra-red fluxes and cooling rates at various levels of the atmosphere as obtained from the two methods, to examine the order of agreement, and to seek an explanation of the differences.

2. Radiometersonde observations at Poona

Srivastava *et al.* (1969) have presented detailed results of a large number of radiometersoundings made at Poona during the years 1963 to 1966. The soundings were made generally once a week, the observation time being around 2000 IST. The data presented comprise air temperature, dewpoint temperature, upward, downward and net infra-red fluxes, and the rate of heating (cooling) at 50 mb interval from the surface to 200 mb and at 25 mb interval thereafter. The instrumentation employed was the Suomi-Kuhn radiometer, which has been described by Suomi *et al.* (1958).

If the ozone, carbon dioxide and cloud distributions are known, the reported air temperatures and dew-points can be made use of to compute the infra-red fluxes at various levels in the atmosphere, which can then be directly compared with the observed fluxes. However, for the purpose of the present work, only those observations made on cloud-free nights were selected, since exact information regarding the heights and amounts of various cloud layers present at the time of observation was not available. The soundings chosen were further grouped together seasonwise as follows —

Season	Months	Number of soundings
Summer	Mar—May	21
Monsoon	Jun—Sep	4
Post-monsoon	Oct—Nov	11
Winter	Dec—Feb	15

Seasonal averages of the observed upward, downward and net infra-red fluxes at the various levels were then derived, and these are plotted in Figs. 1 to 4. The predominant feature of the flux distributions is that both the upward and downward fluxes decrease rapidly from the surface upwards to the 200-mb level, above which the

TABLE 1

Computed values of fluxes and cooling rate at various levels in summer(March-May)

P (mb)	H_2O	CO_2	O_3	Total*	H_2O	CO_2	O_3	Total
	Upward flux (1y/day)				Downward flux (1y/day)			
0	710·9	157·7	80·6	593·5	0·0	0·0	0·0	0·0
25	710·6	156·9	86·2	598·0	4·8	7·1	3·0	15·0
50	710·3	154·7	93·0	602·2	8·1	11·8	3·9	23·9
75	710·3	153·4	96·7	604·7	9·2	12·9	3·9	26·0
100	710·6	154·8	98·9	608·5	9·8	13·3	3·8	27·0
125	711·0	157·8	99·7	612·7	11·7	15·3	3·8	30·9
150	711·9	161·1	100·4	617·6	16·2	18·4	3·9	38·5
175	713·4	164·5	100·9	623·0	23·6	21·7	3·9	49·3
200	715·7	168·1	101·4	629·5	34·6	25·6	4·0	64·3
250	724·1	175·9	102·3	646·6	64·1	34·2	4·3	102·7
300	735·2	183·0	103·0	665·4	97·8	42·9	4·5	145·4
350	749·1	190·0	103·6	687·0	132·9	51·4	4·8	189·3
400	766·0	197·3	104·1	711·6	168·9	60·6	5·1	234·7
450	783·1	203·8	104·5	735·6	204·7	69·6	5·4	279·7
500	799·5	209·4	104·8	757·9	239·5	78·0	5·7	323·3
550	814·5	214·3	105·1	778·2	271·9	85·3	6·0	363·3
600	832·3	219·6	105·4	801·5	305·9	92·7	6·2	404·9
650	852·2	225·3	105·6	827·3	339·2	100·5	6·5	446·3
700	874·0	231·0	105·8	855·0	373·9	108·4	6·8	489·3
750	895·9	236·4	105·9	882·5	409·2	116·6	7·2	533·1
800	915·6	241·1	106·1	907·1	442·8	124·4	7·6	574·9
850	932·4	245·0	106·2	927·9	473·8	131·7	8·1	613·7
900	943·4	247·4	106·3	941·3	500·5	137·6	8·7	646·9
946	954·0	249·4	106·3	954·0	530·3	143·0	9·3	682·7
	Net flux (ly/day)				Heating rate (°C/day)			
0	710·9	157·7	80·6	593·5				
25	705·7	149·7	83·1	582·9	—0·849	—1·296	0·411	—1·733
50	702·1	142·9	89·0	578·3	—0·592	—1·129	0·962	—0·759
75	701·1	140·5	92·8	578·6	—0·166	—0·392	0·622	0·063
100	700·7	141·5	95·0	581·5	—0·063	0·162	0·367	0·465
125	699·3	142·4	95·8	581·8	—0·233	0·161	0·125	0·048
150	695·6	142·7	96·4	579·0	—0·599	0·041	0·106	—0·451
175	689·7	142·7	97·0	573·7	—0·968	0·002	0·085	—0·880
200	681·0	142·5	97·4	565·2	—1·429	—0·031	0·068	—1·392
250	660·0	141·6	98·0	543·8	—1·723	—0·075	0·050	—1·748
300	637·3	140·0	98·4	520·0	—1·860	—0·132	0·036	—1·956
350	616·2	138·5	98·8	497·7	—1·731	—0·122	0·026	—1·827
400	597·1	136·6	99·0	476·9	—1·566	—0·151	0·016	—1·702
450	578·4	134·1	99·1	455·8	—1·536	—0·205	0·007	—1·734
500	559·9	131·4	99·1	434.6	—1·512	—0·227	0·003	—1·736
550	542·6	128·9	99·1	414·8	—1·422	—0·201	0·000	—1·623
600	526·4	126·9	99·1	396·5	—1·327	—0·167	—0·002	—1·497
650	512·9	124·8	99·0	380·9	—1·102	—0·170	—0·005	—1·278
700	500·0	122·5	98·9	365·7	—1·056	—0·188	—0·009	—1·253
750	486·6	119·8	98·7	349·4	—1·098	—0·221	—0·015	—1·335
800	472·8	116·7	98·4	332·2	—1·136	—0·253	—0·023	—1·412
850	458·6	113·2	98·0	314·1	—1·159	—0·285	—0·031	—1·476
900	442·8	109·8	97·5	294.4	—1·298	—0·284	—0·041	—1·623
946	423·7	106·3	97·0	271·2	—1·683	—0·301	—0·048	—2·033

*Note—While summing up the upward flux for the three gases at any level, the terms b for CO_2 and Ozone are not considered as they are included in the term πB [See equations (2) and (4)]

rate of decrease becomes small or even negative. The net flux, which is the difference between the fluxes in the two directions, however, increases with height up to 200 mb, remains practically steady between 200 and 75 mb, and increases again rather rapidly with height above 75 mb. In the monsoon season, however, the net flux shows a marked fall from 200 to 75 mb.

The vertical profiles of the radiative heating rate (Figs. 5 to 8) show that in all the four seasons the troposphere (surface to 200 mb) experiences a cooling. This may be expected, since the observations chosen have been made only on those days when the cloud amount reported was zero. In winter and summer, the variation of $\partial T/\partial t$ with height in the troposphere is confined to a rather narrow range, the cooling rates being about 1 to 2·5°C/day. In the monsoon and post monsoon seasons, however, wide fluctuations of cooling rate (0·2 to 4·6°C/day) are observed in the troposphere. Another feature which is exhibited by the cooling rate patterns all through the year is a large cooling (>4°C/day) in the stratosphere. Between 50 and 200-mb levels, $\partial T/\partial t$ exhibits a lot of variation with respect to season in addition to that with height. For exampe, at 137·5 mb, $\partial T/\partial t$ has a value of +6·4°C/day during the monsoon and —2·4°C/day in summer.

3. Numerical computations of infra-red flux

The fluxes of infra-red radiation in the downward and upward directions at any given level k of the atmosphere are evaluated from the following equations :

(*a*) For water vapour,

$$\overset{\downarrow}{F}_k = \pi B_c \bar{\epsilon}_f(y_o, T_c) - \int_{B_o}^{B_c} \bar{a}_f(y_o, T)\,\pi dB - \int_{B_k}^{B_o} \bar{a}_f(y, T)\,\pi dB \qquad (1)$$

$$\overset{\uparrow}{F}_k = \pi B_* - \int_{B_k}^{B_*} \bar{a}_f(y, T)\,\pi dB \qquad (2)$$

(*b*) For carbon dioxide and ozone,

$$\overset{\downarrow}{F}_k = \pi b_c \bar{A}_f(y_o, T) - \int_{b_k}^{b_o} \bar{A}_f(y, T)\,\pi db \qquad (3)$$

$$\overset{\uparrow}{F}_k = \pi b_* - \int_{b_k}^{b_*} \bar{A}_f(y, T)\,\pi db \qquad (4)$$

The net flux is given by,

$$F_k^{\text{net}} = \overset{\uparrow}{F}_k - \overset{\downarrow}{F}_k \qquad (5)$$

and the rate of heating is given by the flux divergence equation,

$$\frac{\partial T}{\partial t} = \frac{g}{c_p}\frac{\partial F^{\text{net}}}{\partial p} \qquad (6)$$

Here, B_o, B_k, B_* are the black-body fluxes at the temperatures prevailing at the top of the atmosphere at level k and the surface respectively; b_o, b_k, b_* are the corresponding black-body fluxes within the carbon dioxide or ozone band limits; B_c is the black-body flux at a temperature T_c introduced for the convenience of integration; y refers to the optical depth and y_o to the optical depth with respect to the top of the atmosphere; $\bar{a}_f$ and $\bar{\epsilon}_f$ are the mean slab absorptivity and emissivity of water vapour and $\bar{A}_f$ is the mean slab absorptivity of carbon dioxide or ozone.

The finite difference scheme for solving equations (1) to (4) has been described in detail by the authors in an earlier work (Godbole, Kelkar and Murakami 1970).

The numerical scheme described above was used to compute infra-red fluxes in the upward and downward directions at the same levels at which the radiometersonde observations were available, *viz.*, at 50 mb interval below 200 mb and at 25 mb interval above 200 mb. The contributions of all the three gases, *i.e.*, water vapour, carbon dioxide and ozone were considered and summed up. For this purpose, the water vapour distributions in the vertical were constructed from the mean dew-point profile for each season obtained from the radiometersonde data. The carbon dioxide mixing ratio was assumed to be constant, and the ozone distribution was derived from ozonesonde observations over Poona (Mani and Sreedharan 1969). Seasonal averages of temperature at various levels obtained from the radiometer soundings were used in the computations.

4. Comparison of observed and computed fluxes and cooling rates

The vertical distributions of upward, downward and net fluxes and the heating rate in the four different seasons as obtained from computations are shown in Figs. 1 to 8 alongside the observed distributions for ease of comparison. The individual contributions of water vapour, carbon dioxide and ozone have been given in Table 1 for one season (summer).

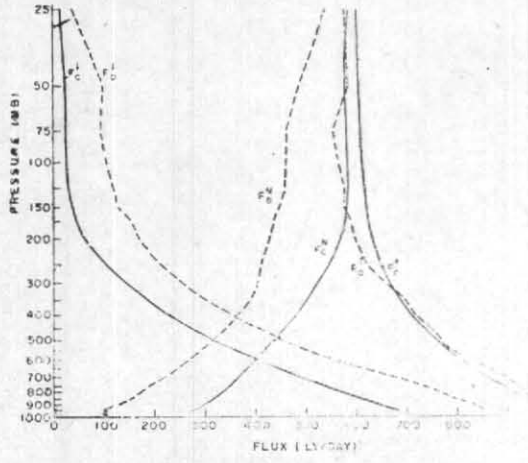

Fig. 1. Summer (Mar—May)

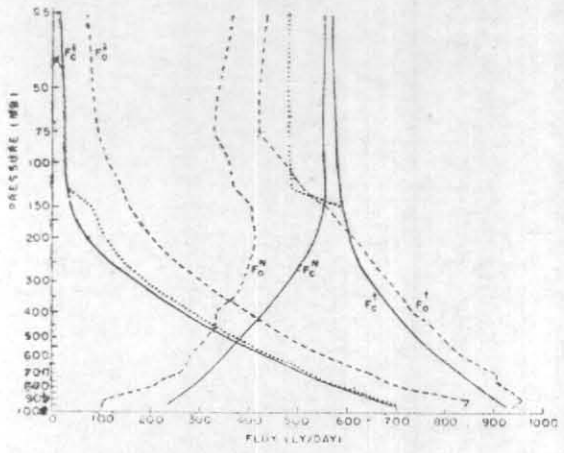

Fig. 2. Monsoon (June—Sep)

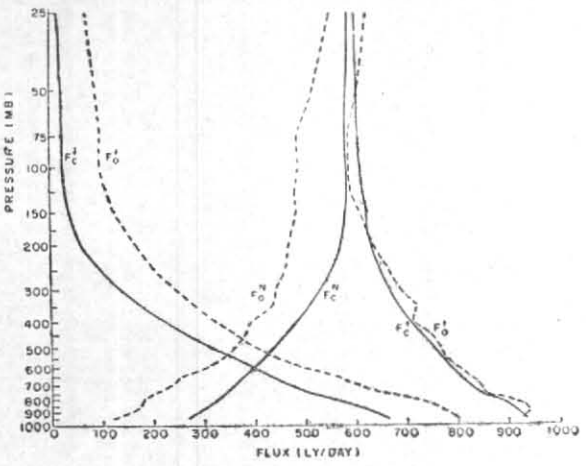

Fig. 3. Post monsoon (Oct—Nov)

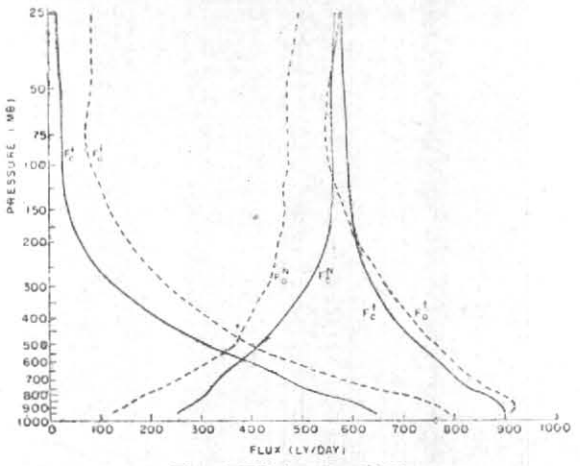

Fig. 4. Winter (Dec-Feb)

Figs. 1-4. vertical distribution of upward, downward, and net fluxes
Solid line—Computed, Dashed lines—Observed

(a) *Upward flux*:—It is observed that (Figs. 1-4) the computed values of upward flux are in fairly close agreement with the observed ones in all seasons, except the monsoon. However, the computed value is generally less than the observed value in the lower troposphere, whereas the reverse is observed in the upper troposphere and stratosphere. The difference between the computed and observed upward fluxes is of the order of 10 per cent or less. However, during the monsoon season, much larger discrepancies are noticeable in the region above the 100-mb level.

(b) *Downward flux*—The variations of the computed values of the downward flux with respect to height and season are seen to be of a similar nature as the variations of the observed downward flux values. However, although the observed and computed curves run almost parallel, at any given level the observed flux appears to exceed the computed flux by a large amount of the order of 75 to 150 ly/day.

(c) *Net flux*—The differences between the computed and observed values of the net flux are of an opposite nature compared to those between the downward fluxes, as a result of the situation that the upward fluxes are in fair agreement. Thus the observed net flux is always smaller than the computed one by about 100-150 ly/day. During the monsoon, discrepancies as large as 200 ly/day are observed in the stratosphere.

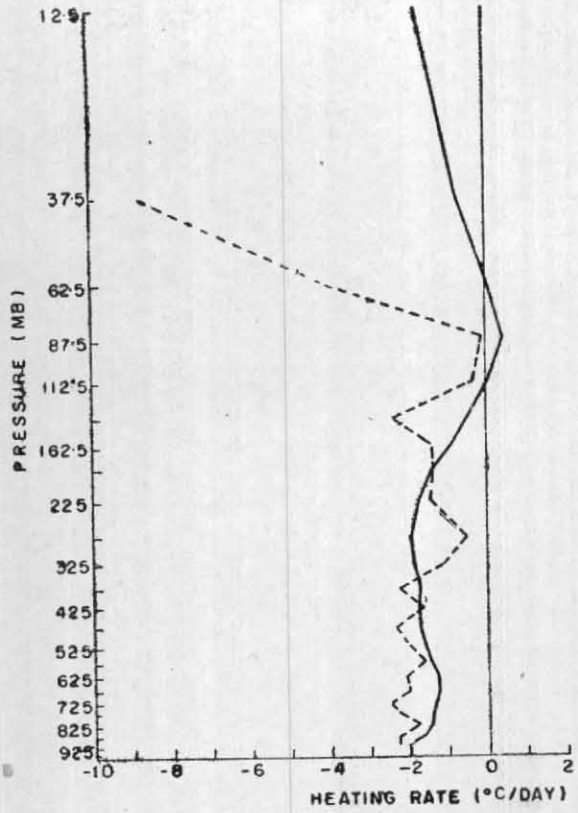

Fig. 5. Summer (Mar—May)

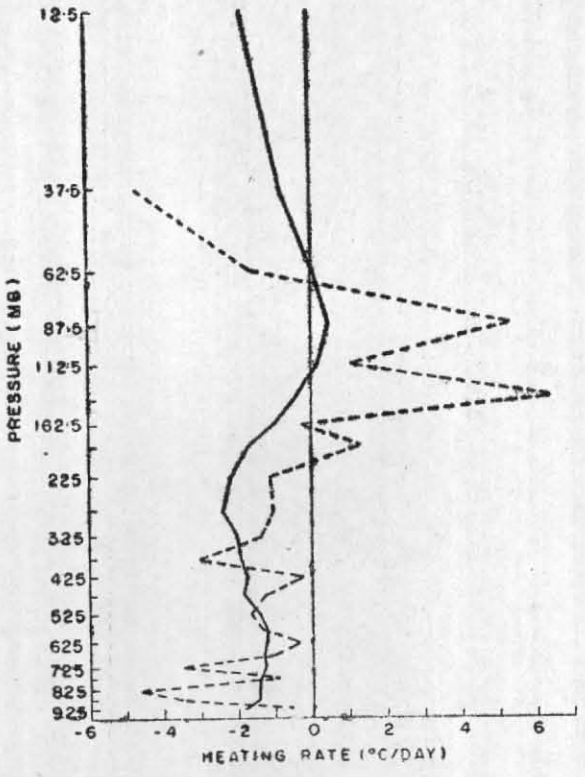

Fig.6. Monsoon (Jun—Sep)

Vertical distribution of heating

Solid lines—Computed values Dashed lines—Observed values

(d) *Heating rate*—The computed heating rate in the troposphere always exhibits negative values, *i.e.*, cooling (1 to 2°C/day) and agrees with the observations. However, the fluctuating nature of the observed cooling in the troposphere during the monsoon and post monsoon is not reflected on the computed curve. The agreement between observations and computations is quite good, considering the fact that the cooling rate is an extremely sensitive parameter. For example, the cooling rate of a 50 mb thick layer of the atmosphere could change by 0·4°C/day if the difference in net flux across the layer is in error by 5 ly/day (*vide* Eq. 6).

Above and near the tropopause, there are significant differences between the observed and computed cooling rates. In the stratosphere, the observed cooling rate is quite large in all seasons (4 to 9 °C/day at 37·5 mb) whereas the computed value at that level is less than 1 °C/day. Near 100 mb the computed value falls between ±0·5 °C/day whereas the heating observed varies between + 6° and —4 °C/day.

5. Discussion

Suomi *et al.* (1958) have described the construction of the Suomi-Kuhn radiometer and the possible errors in the measurement of flux. They have concluded that the errors tend to reduce the temperature difference across the radiometer surfaces, and accordingly, the downward flux is overestimated, while the upward flux is underestimated. This results in the net flux being underestimated. Instrumental errors may therefore partially account for the discrepancies noticed between the computed and observed fluxes. However, it is highly unlikely that discrepancies of the order of 75 to 150 ly/day in the downward flux could be attributed to instrumental errors alone. Besides, such comparisons made with other types of ground-based instrumentation have also shown the observed downward flux at the surface to be higher than the computed one (Robinson 1947, Mani *et al.* 1965).

Kelkar and Godbole (1970) have shown that the upward flux at any given level is strongly

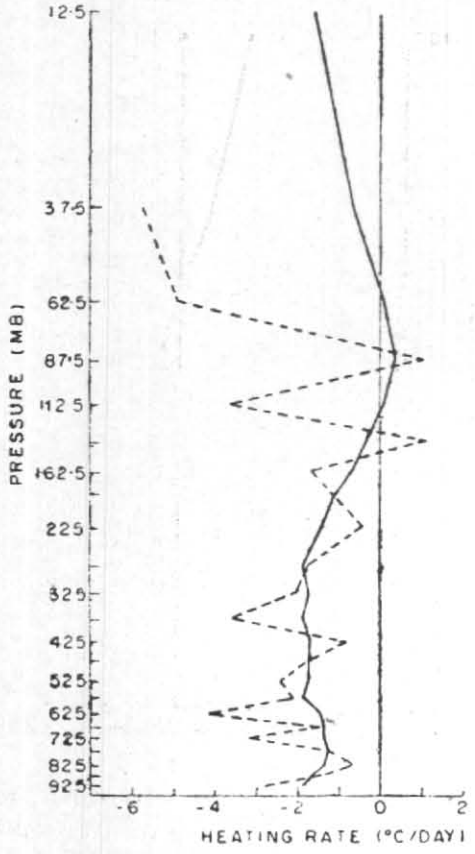

Fig. 7. Post monsoon (Oct—Nov)

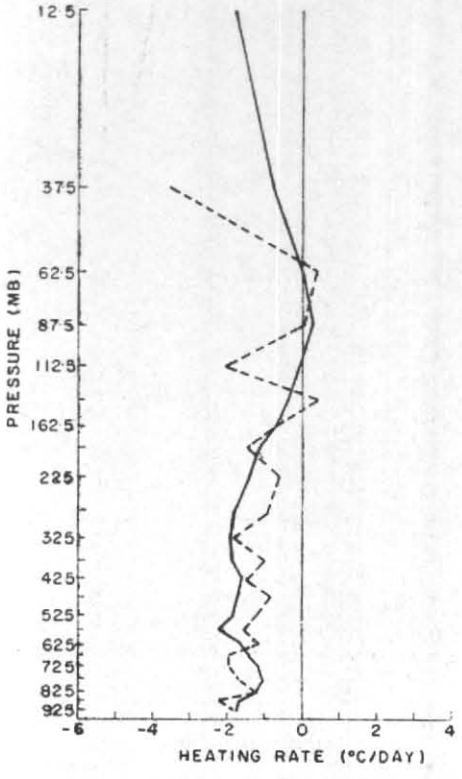

Fig. 8. Winter (Dec—Feb)

Vertical distribution of heating rate

Solid lines — Computed values Dashed lines — Observed values

controlled by the ground temperature, while the downward flux is dependent on the absorber concentration above the level. The good agreement noticed between observed and computed values of the upward flux is thus explainable. On the other hand, the computed value of the downward flux could be in error if the absorber distribution, especially that at higher levels in the stratosphere, has not been properly understood. As revealed by the computations (Table 1) the contribution of ozone to the total downward flux at any level is less than 10 ly/day, which means that errors in the ozone distribution are not very important. As regards carbon dioxide, the mixing ratio is considered to remain constant till at least 60-70 km height. It is thus very important to have accurate measurements of water vapour mixing ratio in the stratosphere. It is also essential to determine the contribution of aerosols to infra-red radiation and to obtain vertical profiles of aerosol concentrations. Frequent occurrences of aerosol layers upto heights of 29 km have been reported by Kondratyev (1970). On the other hand, it would be worthwhile to have radiometersonde measurements above 25 mb to determine whether the downward flux tends to zero with increasing height. If the measurements do not show such a tendency, the shift between the observed and computed values of the downward flux may not be related to physical causes, but could be the effect of erroneous instrumental behaviour.

The differences between the observed and computed values of the cooling rate in the stratosphere could likewise be attributed to possible errors in the water vapour distribution assumed and to the fact that the presence of aerosols was not considered. However, while explaining the discrepancies in the cooling rates in the troposphere, particularly in the monsoon season, the possibility of the presence of thin clouds not observable from the ground could not be ruled out, especially since the observations were made at night hours. From this point of view, the computations were reperformed for the monsoon season with two hypothetical situations. In the first case, a cloud layer was introduced with base at 150 mb and top at 125 mb and having a small horizontal

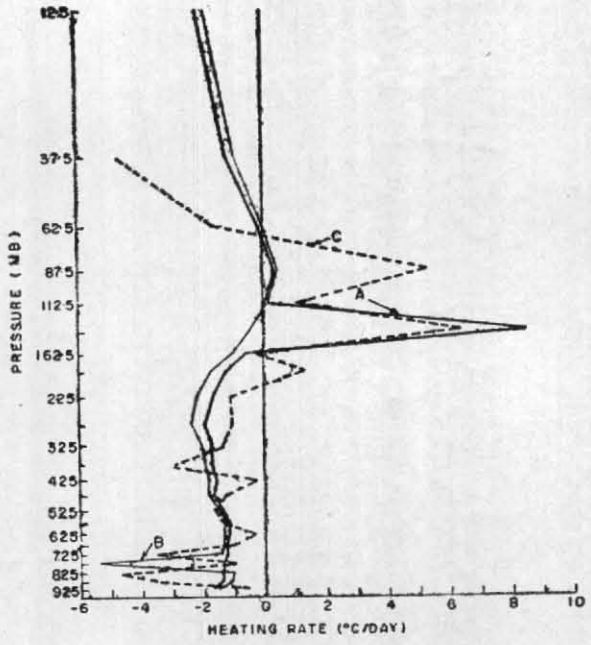

Fig. 9

Computed heating rate for (A) cloud of 2 octas between 125-150 mb; (B) cloud of 2 octas between 750-800 mb, other conditions being as in monsoon (Jun-Sep) and curve (C) is observed heating rate for the season

extent of 2 octas. In the second case, a cloud layer was as umed to exist between 750 and 800 mb, the cloud amount being 2 octas again. For the purpose of these additional computations involving the presence of cloud, the computation scheme of Section 3 had to be modified.

In the case of an overcast sky, equations (1) and (2) were modified as follows, under the assumption that the cloud layer can be approximated as a black-body.

(a) Above the cloud top,

$F_k^{\downarrow}$ is given by equation (1).

$$F_k^{\uparrow} = \pi B_{\text{top}} - \int_{B_k}^{B_{\text{top}}} \bar{a}_f(Y,T)\, \pi\, dB \qquad (7)$$

(b) Within the cloud layer,

$$F_k^{\downarrow} = F_k^{\uparrow} = \pi B_k \qquad (8)$$

(c) Below the cloud base,

$$F_k^{\downarrow} = \pi B_{\text{base}} - \int_{B_k}^{B_{\text{base}}} \bar{a}_f(Y,T)\, \pi\, dB \qquad (9)$$

$F_k^{\uparrow}$ is given by Eq. (2).

Here B_{base} and B_{top} are the black body fluxes at the cloud base and top temperatures resepectively. In the case of carbon dioxide and ozone, equations (3) and (4) were modified in a similar manner. The fluxes and cooling rates corresponding to the partial cloud cover assumed were prorated from their values in the clear sky and overcast situations.

From the results of these computations, it is seen that (Fig. 9) the thin low cloud (750-800 mb, 2 octas) leads to infra-red cooling of 5·4° C/day at 775 mb, whereas the thin high cloud (125-150 mb, 2 octas) produces infra-red warming of 8·5° C/day at 137·5 mb. The order of magnitude of this cooling (warming) agrees very well with the observations in the lower (upper) troposphere, thus indicating a strong likelihood of tenuous clouds in the atmosphere at the time of observation.

The vertical profiles of the observed and computed infra-red fluxes also tend to come closer when a thin cloud is introduced as described above. The change in the upward and downward flux that takes place when the high cloud is considered is shown in Fig. 2. It is clearly seen that the difference noticed in the high atmosphere between the observed and computed fluxes in the upward direction narrows down considerably, compared to the clear sky case. As regards the

downward fluxes, the discrepancies are also found to reduce, although to a smaller extent.

6. Conclusion

(1) The study has shown that the observed and computed values of the upward flux agree well at all levels of the atmosphere, the difference being less than 10 per cent.

(2) The downward flux at any level is observed to be higher than the computed value by 75 to 150 ly/day. The nature of variation with height is, however, the same in both the observed and computed cases. This discrepancy is partially attributable to instrumental errors, and also points out the need for accurate measurements of water vapour and aerosols in the stratosphere.

(3) The order of magnitude of the observed and computed heating rates agrees in the troposphere. However, the computed results do not show the large values of cooling observed in the stratosphere and the zigzag nature of the cooling rate observed in the troposphere during monsoon and post monsoon. The difference could be due to the presence of thin cloud layers in the atmosphere not observable from the ground.

Acknowledgements — The authors are thankful to Dr. Bh. V. Ramana Murty for his interest in the study, for going through the manuscript and for making useful suggestions. Thanks are also due to our colleagues in the Drawing Section for preparing the diagrams.

REFERENCES

Godbole, R .V., Kelkar, R. R. and Murakami, T.	1970	*Indian J. Met. Geophys.*, **21**, pp. 43-52.
Kelkar, R. R., and Godbole, R. V.	1970	*Ibid.*, **21**, 4, pp. 613-622.
Kondratyev, K. Ya., Badinov, I. Ya, Ivlev, L. S. and Nikolsky, G. A.	1970	*W.M.O. Tech. Note* No. 104, pp. 244-245.
Mani, A., Chacko, O. and Iyer, N. V.	1965	*Indian J. Met. Geophys.*, **16**, pp. 445-452.
Mani, A. and Sreedharan, C. R.	1969	*Ann. Geophys.*, **25**, pp. 173-181.
Robinson, G. D.	1947	*Quart. J. R. met. Soc.*, **73**, pp. 127-150.
Srivastava, G. P. and Srinivasan, V.	1969	*India met. Dep. Sci. Rep.* No. 85, 123 pp.
Suomi, V. E., Staley, D. O. and Kuhn, P. M.	1958	*Quart. J. R. met. Soc*, **84**, pp. 134-141.